Technical Note

Water–Fat Separation With IDEAL Gradient-Echo Imaging

Scott B. Reeder, MD, PhD,[1,2]* Charles A. McKenzie, PhD,[3] Angel R. Pineda, PhD,[4] Huanzhou Yu, PhD,[5] Ann Shimakawa, MS,[5] Anja C. Brau, PhD,[5] Brian A. Hargreaves, PhD,[4] Garry E. Gold, MD,[4] and Jean H. Brittain, PhD[6]

Purpose: To combine gradient-echo (GRE) imaging with a multipoint water–fat separation method known as "iterative decomposition of water and fat with echo asymmetry and least squares estimation" (IDEAL) for uniform water–fat separation. Robust fat suppression is necessary for many GRE imaging applications; unfortunately, uniform fat suppression is challenging in the presence of B_0 inhomogeneities. These challenges are addressed with the IDEAL technique.

Materials and Methods: Echo shifts for three-point IDEAL were chosen to optimize noise performance of the water–fat estimation, which is dependent on the relative proportion of water and fat within a voxel. Phantom experiments were performed to validate theoretical SNR predictions. Theoretical echo combinations that maximize noise performance are discussed, and examples of clinical applications at 1.5T and 3.0T are shown.

Results: The measured SNR performance validated theoretical predictions and demonstrated improved image quality compared to unoptimized echo combinations. Clinical examples of the liver, breast, heart, knee, and ankle are shown, including the combination of IDEAL with parallel imaging. Excellent water–fat separation was achieved in all cases. The utility of recombining water and fat images into "in-phase," "out-of-phase," and "fat signal fraction" images is also discussed.

Conclusion: IDEAL-SPGR provides robust water–fat separation with optimized SNR performance at both 1.5T and 3.0T with multicoil acquisitions and parallel imaging in multiple regions of the body.

Key Words: fat suppression; chemical shift imaging; gradient echo; magnetic resonance imaging; water–fat separation; IDEAL; hepatic steatosis
J. Magn. Reson. Imaging 2007;25:644–652.

GRADIENT-ECHO (GRE) imaging is a rapid MRI method that is used for a variety of applications throughout the body. T_1-weighted (T_1W) spoiled gradient-echo (SPGR) sequences are of particular importance for postcontrast imaging in many areas of the body, including the abdomen (1) and breast (2). Noncontrast-enhanced T_1W SPGR imaging is also highly valuable for assessing cartilage morphology (3).

Many T_1W GRE imaging applications require suppression of fat signal. Fat is bright in these sequences and can potentially obscure underlying pathologies, such as tumor or inflammation. Unfortunately, reliable and uniform fat suppression can be challenging in areas of main field (B_0) and RF (B_1) inhomogeneities. Examples of challenging applications include imaging of the extremities and areas with unfavorable geometry (e.g., the brachial plexus), off-isocenter imaging, and large field of view (FOV) imaging. Other fat-suppression methods, such as short TI inversion recovery (STIR) (4), are incompatible with rapid GRE imaging because of the need for a long inversion time (approximately 200 msec). Spectral-spatial or water-selective pulses can be combined with GRE imaging, but they are lengthy. Although the fat–water discrimination achieved by these pulses is insensitive to B_1 inhomogeneities, they are still sensitive to B_0 inhomogeneities (5).

In 1984 Dixon (6) first described "in- and out-of-phase" imaging, a method that acquires two images at different echo times (TEs), thereby exploiting the difference in chemical shift between water and fat, facilitating the separation of these species into different images. Glover (7) further refined this approach in 1991 with a "three-point" method that removed the effects of B_0 field

[1]Department of Radiology, University of Wisconsin, Madison, Wisconsin, USA.
[2]Department of Medical Physics, University of Wisconsin, Madison, Wisconsin, USA.
[3]Department of Radiology, Beth Israel-Deaconess Medical Center, Boston, Massachusetts, USA.
[4]Department of Radiology, Stanford University Medical Center, Stanford, California, USA.
[5]Applied Science Lab-West, GE Healthcare, Menlo Park, California, USA.
[6]Applied Science Lab, GE Healthcare, Madison, Wisconsin, USA.
Contract grant sponsor: Lucas Foundation; Contract grant sponsor: GE Healthcare; Contract grant sponsor: National Institutes of Health; Contract grant numbers: P41-RR09784; RO1-EB002524.
*Address reprint requests to: S.B.R., Department of Radiology, E3/311 CSC, University of Wisconsin, 600 Highland Ave., Madison, WI 53792-3252. E-mail: sreeder@wisc.edu
Received November 1, 2005; Accepted September 28, 2006.
DOI 10.1002/jmri.20831
Published online in Wiley InterScience (www.interscience.wiley.com).

inhomogeneities by acquiring a third image. Numerous variations of these methods have since been described for the separation of water and fat (8–10).

Although the primary advantage of these methods is that they minimize the effects of B_0 inhomogeneities, water–fat separation methods, unlike other fat-suppression methods, also have the unique ability to provide both water *and* fat images from the same acquisition. This permits quantification of water and fat within a voxel and enhanced characterization of tissue through direct visualization of fatty tissue in addition to tissue with water signal.

Recently, Pineda et al (11) performed the first comprehensive noise analysis of three-point water–fat separation methods. They demonstrated that the theoretical optimal combination of echoes for a three-point fast spin-echo (FSE) acquisition occurred when the phase between water and fat phase was $-\pi/6,\pi/2,7\pi/6$. This combination of echoes was applied to FSE imaging using an iterative least-squares water–fat separation method that allowed for arbitrarily and unequally spaced echo shifts (9). Experimental validation of the noise performance showed that the maximum possible SNR of the FSE water and fat images was achieved (12). This method has been applied to various FSE applications, including the ankle, brachial plexus, and cervical spine (13,14), as well as balanced steady-state free precession (SSFP) imaging in the knee (9) and heart (15).

The theoretical noise behavior predicted by Pineda et al (11) has not been experimentally validated for GRE imaging. Validation of the noise behavior for GRE imaging is important because the overall predicted noise behavior for GRE imaging is different from that for either FSE or SSFP imaging (11). It can be shown that the optimum choice of echoes that maximizes the noise performance of magnitude images leads to lower noise performance for the phase and field maps for GRE imaging, compared to FSE or SSFP (11). This is related to the fact that all echo shifts for GRE imaging must be greater than zero, while echo shifts can be negative for FSE because echoes can be acquired before the refocusing of the spin echo. This effect also occurs with SSFP because of the 180° relative phase shift between water and fat at TE = TR/2 for certain choices of TR. Therefore, experimental validation of the noise performance for IDEAL-GRE imaging is necessary in order to show that the optimum noise performance is achievable even in the presence of higher uncertainty in the phase and field maps.

The purpose of this work was to combine IDEAL with GRE imaging at 1.5T and 3.0T. Experimental validation of the noise performance of the water–fat separation was performed to optimize the noise performance and overall image quality. Clinical results, including examples of imaging in the liver, breast, knee, ankle, and heart, are shown. Finally, the recombination of water and fat images in new ways, such as "fat fraction" images, are described, and may be helpful for the quantification of fatty infiltration or other pathologies.

MATERIALS AND METHODS

Theory

Noise Performance

As described previously (7), the noise performance of a water–fat decomposition is conveniently described with the effective number of signal averages (NSA), defined as

$$NSA = \frac{\sigma^2}{\sigma_\rho^2} \qquad (1)$$

where σ^2 is the variance of the noise in a source image, and σ_ρ^2 is the variance of the noise in a calculated water or fat image. The NSA is a useful measure of the noise performance of a water–fat decomposition, and has an intuitive basis: for any three-point water–fat decomposition method, the maximum possible NSA is three, which is equivalent to what would be obtained if the object contained only water or only fat, and the three source images were averaged (7). Equation [1] will be used experimentally to determine the noise performance of the IDEAL-GRE method.

Optimal Echo Shifts

The phase shift between water and fat from an echo acquired at time t relative to TE = 0, can be written as

$$\theta = 2\pi\Delta f\, t \qquad (2)$$

where Δf is the chemical shift between water and fat (–210 Hz at 1.5T, and –420 Hz at 3.0T). Phase shifts are more convenient than echo shifts because they are independent of field strength and are more intuitive, and thus give more physical meaning to the water–fat separation problem.

As predicted by Pineda et al (11), one set of optimal echo shifts for the three images occur when the water–fat phase is

$$\begin{aligned} &1^{\text{st}}\text{ echo: } -\pi/6 + \pi k \\ &2^{\text{nd}}\text{ echo: } \pi/2 + \pi k \\ &3^{\text{rd}}\text{ echo: } 7\pi/6 + \pi k,\ k = \text{any integer} \end{aligned} \qquad (3)$$

This echo combination has an intuitive basis as follows: In the "perfect" NMR experiment, there are no constant phase shifts or B_0 inhomogeneities, and an image acquired with a TE that has water and fat in quadrature, i.e., $\pi/2 + \pi k$, can be used to separate water from fat with that single image. Water and fat are simply the real and imaginary components of the complex image. However, the presence of unknown constant phase shifts and B_0 inhomogeneities requires additional information. The acquisition of two additional images 120° ($2\pi/3$) before and after the second echo located at $\pi/2+\pi k$ provides uniform sampling around the unit circle, and thus yields optimal noise performance in the estimation of water and fat from the three source images. It is important to note that the center echo must

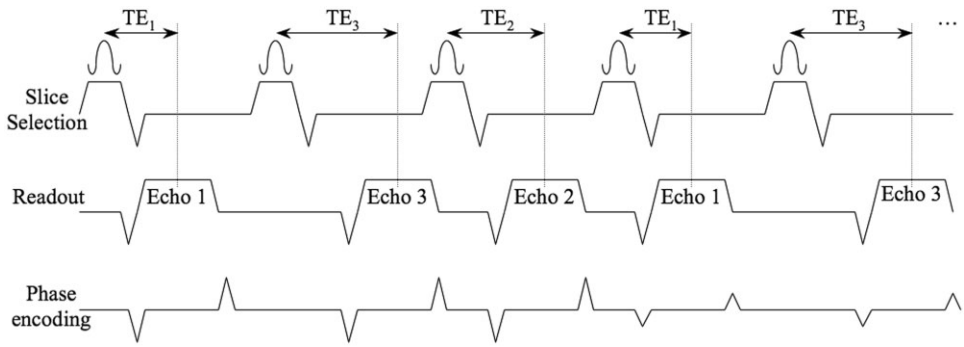

Figure 1. Pulse sequence diagram of a 2D-IDEAL-GRE acquisition. For each phase-encoding step, three echoes are acquired in an interleaved manner to prevent misregistration due to motion or other physiologic processes. The echoes are ordered TE_1, TE_3, TE_2 to prevent the relatively close spacing of the readout gradient that would occur if TE_1 ever followed TE_3. Echo ordering such as this (e.g., TE_1, TE_2, TE_3) can cause additional phase shifts from eddy currents between TRs, leading to ghosting artifacts.

be in quadrature. Echo combinations with the first or third echo in quadrature will not have optimal noise performance (11).

Echo shifts that satisfy Eq. [3] will have optimal noise performance. However, noise performance is poor when the second echo is acquired when water and fat are aligned, i.e., any multiple of 2π, even if the spacing between all three echoes remains at $2\pi/3$. In this case, the NSA = 3 when a voxel contains all water, but is significantly reduced for voxels that contain all fat, and has a broad minimum approaching zero for voxels containing mixtures of water and fat in near equal proportions (11). This echo combination can lead to image artifacts that include irregular margins at the interface between tissues with water signal (e.g., muscle) and fat signal (e.g., subcutaneous fat), as a result of partial-volume effects. In addition, areas of the calculated water image that contain mostly fat signal (e.g., bone marrow and subcutaneous fat) appear noisy (12).

The choice of echo group, determined by the echo group index k, will depend on the minimum TE (TE_{min}) of the sequence. Typically, k is chosen to minimize the TEs, but one must ensure that they are all greater than TE_{min}. For example, at 1.5T one possible echo combination for IDEAL-GRE imaging occurs for $k = 1$, with echo shifts of 2.0 msec, 3.6 msec, and 5.2 msec, so long as TE_{min} is 2.0 msec or less. It is worthwhile to note that spacing between echo groups decreases with increasing field strength: the time between consecutive echo groups at 1.5T is approximately 2.4 msec, compared to a spacing of 1.2 msec at 3.0T. The decrease in time between echo groups, and the fact that echoes within a group are more closely spaced with increasing field strength make IDEAL more flexible and more efficient for imaging at 3.0T.

Pulse Sequence and Image Reconstruction

IDEAL uses an iterative least-squares method that is compatible with multicoil imaging (9). In this method, an iterative method is used to determine the local field map (B_0 inhomogeneity) in the least-squares sense. The field map is subsequently demodulated from the signal in the source images. This signal is then decomposed into separate water and fat signal signals using a least-squares solution matrix inversion. The latter step is similar to the least-squares approach described by An and Xiang (8), which is restricted to equally spaced echo shifts. IDEAL uses a region-growing reconstruction algorithm to prevent water–fat "swaps" that can occur from the natural ambiguity between water and fat signals (16), e.g., for an acquisition at 1.5T with the center frequency set to water, water that is off-resonance by –210 Hz has similar signal to fat that is on-resonance.

In order to reduce the effects of motion and the possibility of misregistration between subsequent echoes, acquisitions at different TEs are interleaved as shown in Fig. 1. For each phase-encoding step, the three echoes were acquired in the following order: TE_1, TE_3, TE_2, TE_1, TE_3, TE_2 . . ., where $TE_1 < TE_2 < TE_3$. In this way the spacing between the readout gradients is the most uniform between subsequent TRs, and prevents the short spacing between TE_3 and TE_1 that would result if the echoes were interleaved in increasing order (i.e., TE_1, TE_2, TE_3, TE_1, TE_2, TE_3. . .). Ghosting artifacts in the phase-encoding direction were occasionally observed in source images when the echoes were interleaved with increasing spacing. Eddy currents generated from the readout gradient were thought to be a likely cause. No artifacts were observed when the proposed echo order was used.

Experimental

Phantom Experiments and Clinical Scanning

All scanning was performed at 1.5T (Signa TwinSpeed; GE Healthcare, Milwaukee, WI, USA) and 3.0T (Signa VH/i; GE Healthcare, Waukesha, WI, USA). Human scanning was performed with the informed consent of the subjects and the approval of our institutional review boards. We used modified 2D- and 3D-GRE pulse sequences to acquire three images with different echo shifts. The phase-encoding gradient was rewound, and RF spoiling was used to prevent coherences in the transverse magnetization for SPGR imaging.

Phantom experiments were performed to validate the noise behavior of the water–fat decomposition. A spherical phantom consisting of peanut oil floating on 0.9% normal saline doped with 5 mM $NiCl_2$ was imaged at

1.5T with the 2D-SPGR pulse sequence. From an axial scout image, a thick slice was oriented through the water–fat interface in order to create a continuum of fat: water ratios. Imaging was performed with a single channel extremity coil and the following parameters: readout matrix dimension (Nx) = 256, phase encoding dimension (Ny) = 256, one excitation, FOV = 24 cm, slice = 10 mm, bandwidth (BW) = ±83.3 kHz, TR = 10.0 msec, and flip angle = 20°. Product automated linear shim routines were used. The flip angle was chosen empirically to produce similar signal intensity from water and fat. Acquisition was performed with IDEAL echoes with the second echo acquired in quadrature ($5\pi/6,3\pi/2,13\pi/6$): TE = 1.98, 3.57, 5.16 msec at 1.5T, and for an "aligned" echo combination ($4\pi/3,2\pi,8\pi/3$): TE = 3.18, 4.76, 6.35 msec. For each echo combination, the acquisition was repeated 256 times (scan time = 32:45 min).

We calculated the NSA for individual pixels based on Eq. [1], by calculating the variance in the signal for each pixel over all 256 source images (σ^2), and the variance for the corresponding pixel over all 256 calculated water images (σ_ρ^2). We calculated the variance of the signal from the source images as the average variance from the three echo shifts. Pixels outside the phantom were excluded using a threshold mask. For each pixel, the fat: water ratio was calculated from the average of all water and the average of all fat images, and scatter plots of measured NSA vs. fat: water ratio were made. All NSA calculations were performed with offline programs written in Matlab 6.0 (Mathworks, Natick, MA, USA).

Knee, ankle, breast, liver, and cardiac images were acquired from healthy volunteers and patients. Numerous examinations were performed, including more than 40 knee, 10 ankle, 20 cardiac, 30 breast, and 30 liver studies. Fat-saturated GRE images were acquired for comparison in many cases. Abdominal imaging was performed using an eight-channel torso phased-array coil, knee and ankle imaging was performed with a product extremity coil, breast imaging was performed with a four-channel dedicated phased-array breast coil, and cardiac imaging was performed using a four-channel phased-array torso coil. Parallel imaging was often performed for abdominal and breast images acquired with phased-array coils to reduce the scan time. Such accelerations were performed with a modified implementation of a image-based unwrapping algorithm (ASSET; GE Healthcare, Waukesha, WI, USA). All water–fat decomposition calculations were performed online with a reconstruction algorithm based on the iterative least-squares algorithm, which can perform multicoil reconstructions (9,16). Specific image parameters for various clinical applications are listed below. For the knee, the imaging parameters were as follows: matrix = 384 × 192 × 50, FOV = 16 cm, slice = 4 mm, TR = 9.57 msec, TE = 3.96/4.76/5.55 msec for the "aligned" combination, TE = 3.37/4.17/4.96 msec for the quadrature combination (k = 3), BW = ±62.5 kHz, and flip angle of 8°. Both aligned and quadrature echo combinations were acquired to demonstrate the importance of noise performance on image quality. Imaging parameters for the ankle imaging at 3.0T included: matrix = 512 × 256 × 60, FOV = 20 cm, slice = 1.5 mm, TR = 9.28 msec, TE = 3.37/4.17/4.96 msec (k = 3), BW = ±62.5 kHz, flip = 8°, and a total scan time of 7:07 min covering the entire ankle with 0.4 × 0.8 × 1.5 mm^3 voxel resolution. Imaging parameters for breast imaging at 1.5T included: matrix = 512 × 256 × 48, FOV = 32 cm, slice = 4 mm, TR = 10.6 msec, BW = ±83 kHz, TE = 4.56/5.36/6.15 msec (k = 4) covering both breasts in 2:10 min using a parallel acceleration factor of 2 with 0.6 × 1.2 × 4 mm^3 resolution. Imaging parameters for the liver acquired at 3.0T included: matrix = 256 × 160 × 16 (interpolated to 32 slices), FOV = 38 × 34 cm, slice = 7 mm (interpolated to 3.5 mm), TE = 2.2/3.0/3.8 msec (k = 2), TR = 6.1 msec, BW = ±83 kHz, 18° flip, and a parallel acceleration of 2, for a total breath-hold time of 21 seconds. Finally, the parameters for cardiac imaging at 1.5T included: matrix = 224 × 128, FOV = 32 cm, slice = 8 mm, BW = ±62.5 kHz, TR = 5.3 msec, and segmentation factor = 16, for a spatial resolution of 1.4 × 2.5 × 8mm^3 and temporal resolution of 85 msec. The TE increment was limited to 1.0 msec, such that the three TEs were 0.96 msec, 1.96 msec, and 2.96 msec. The minimum possible TE values were used in order to shorten TR, which is necessary to obtain all data within a 20–25-second breath-hold, while maintaining reasonable spatial and temporal resolution.

RESULTS

Figure 2a plots the measured values of the effective NSA from the phantom experiment against the fat: water ratio for two sets of echo combinations. Data points plotted in red, acquired with the aligned combination ($4\pi/3,2\pi,8\pi/3$), demonstrate a broad minimum that occurs for pixels that contain similar amounts of water and fat. Data points plotted in blue, acquired with the IDEAL quadrature echo combination ($5\pi/6,3\pi/2,13\pi/6$), show a uniform NSA of approximately 3 for all fat: water ratios. The data from the quadrature case were fitted to the linear equation: NSA = slope*$\log_{10}$ (fat: water ratio) + intercept. The intercept and slope were calculated to be 2.749 ± 0.003, and −0.05 ± 0.002, respectively. This indicates that the slope of the fitted line is flat, and the intercept is close to but slightly lower than the expected maximum of 3.

IDEAL-SPGR knee images acquired with two different echo combinations are shown in Fig. 2c–d, demonstrating image artifacts caused by the NSA performance shown in Fig. 2a, using the aligned echo combination. Irregular margins at the interface between muscle (water signal) and subcutaneous fat are seen in images acquired with the phase of water and fat aligned for the second echo (Fig. 2b). However, images acquired with the phase of water and fat of the second echo in quadrature (Fig. 2c) do not have these artifacts, and have very similar image quality to conventional fat-saturated images that are shown for comparison (Fig. 2d). Image parameters for these acquisitions included: matrix = 384 × 192 × 50, FOV = 16 cm, slice = 4 mm, TR = 9.57 msec, TE = 3.96/4.76/5.55 msec for the "aligned" combination, TE = 3.37/4.17/4.96 msec for the quadrature combination (k = 3), BW = ±62.5 kHz, and flip angle = 8°.

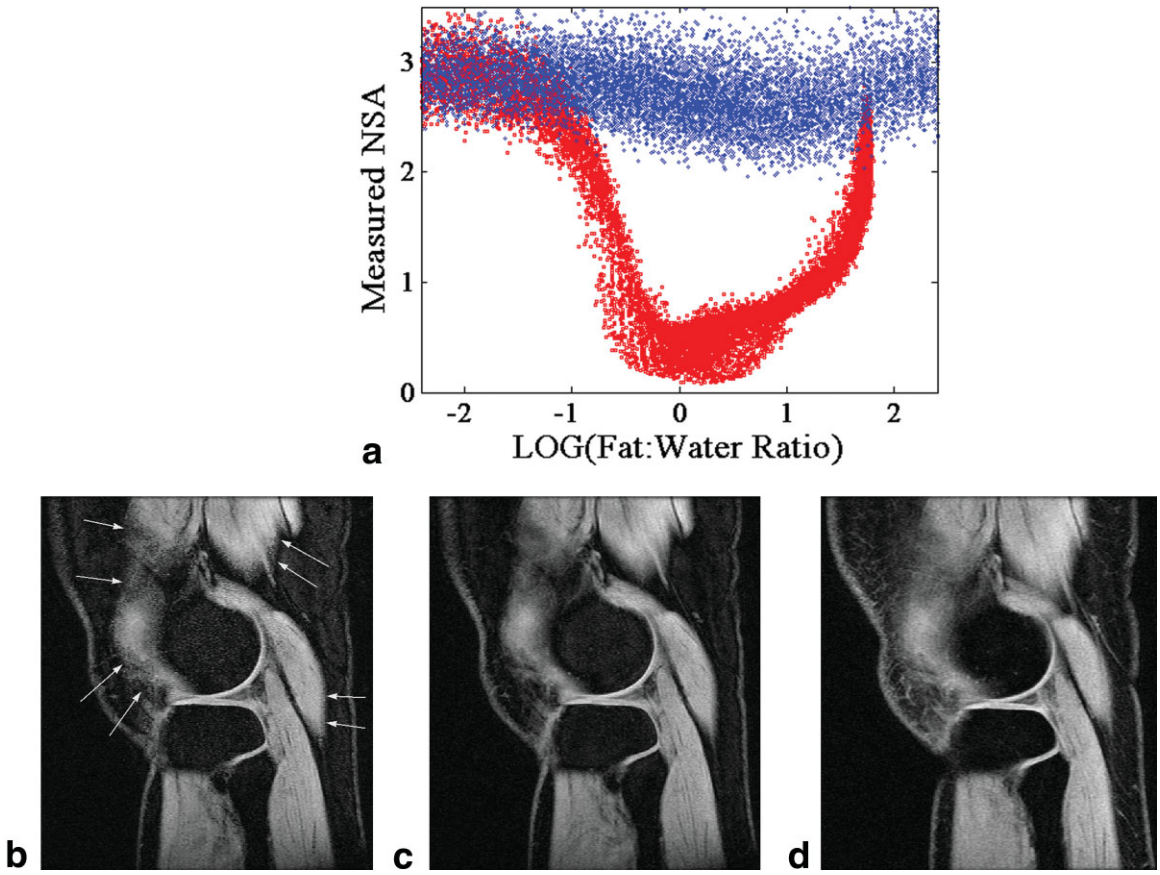

Figure 2. a: Effective NSAs measured from the oil-water phantom with the quadrature echo combination are plotted in blue, and the aligned combination is plotted in red. Close agreement with the expected NSA of 3 for all fat: water ratios was seen with quadrature combination. For the aligned case, a broad minimum that approaches zero is seen when water and fat are in similar proportions within a voxel. The effects of the NSA behavior are seen in calculated water images acquired at 3.0T using 3D-IDEAL-SPGR. The image in **b** was acquired with the aligned echo combination, the image in **c** was acquired with the quadrature echo combination, and a conventional fat-saturated image (**d**) is shown for comparison. Irregular margins between muscle and subcutaneous fat (arrows) are noted with the aligned echo combination, while the quadrature echo combination has very similar image quality compared to the fat-saturated image (d), and is free from the artifacts seen in b.

Examples of high-resolution 3D-IDEAL-SPGR are shown in Fig. 3, including water-only, fat-only, and recombined in-phase and out-of-phase images from the ankle of a normal volunteer and the breasts of another normal volunteer. Excellent depiction of the cartilage of the subtalar and talar joints of the ankle and foot was noted, and uniform separation of water and fat was seen across all images. Uniform suppression was seen across both breasts in all slices.

Images acquired at 3.0T from a patient with fatty infiltration of the liver (hepatic steatosis) are shown in Fig. 4. Fatty infiltration can be visualized as low-level signal in the liver in the fat image, as well as a signal decrease in the calculated out-of-phase image relative to the in-phase image. In addition, a "fat fraction" image displays the proportion of signal from the fat image, calculated on a pixel-by-pixel basis as fat/(water+fat).

Finally, Fig. 5 shows cardiac CINE 2D-IDEAL-SPGR images acquired at 1.5T during breath-holding in a healthy volunteer. Only three of 20 acquired time frames (end-diastole, mid-systole, and end-systole) are shown.

DISCUSSION

In this work we have described an optimized multipoint water–fat separation method known as IDEAL, combined with GRE imaging. By using optimized echo shifts in which the phase shift between water and fat of the central echo is in quadrature ($\pi/2+\pi k$), and the first and third echoes are acquired $2\pi/3$ before and after the central echo, respectively, one can achieve maximal SNR performance. These combinations of echoes also avoid image artifacts that are related to the noise performance of all water–fat separation methods, which in general depends on the water/fat composition of a voxel.

Noise behavior, as quantified experimentally with the NSA, showed good agreement with theoretical predictions. The experimental data for the quadrature echo combination were in close agreement with the predicted theoretical maximum of 3, and high SNR performance was obtained with all fat/water combinations. A marked decrease in noise performance was seen for intermediate combinations of water and fat. The qualitative behavior was very similar to that seen previously

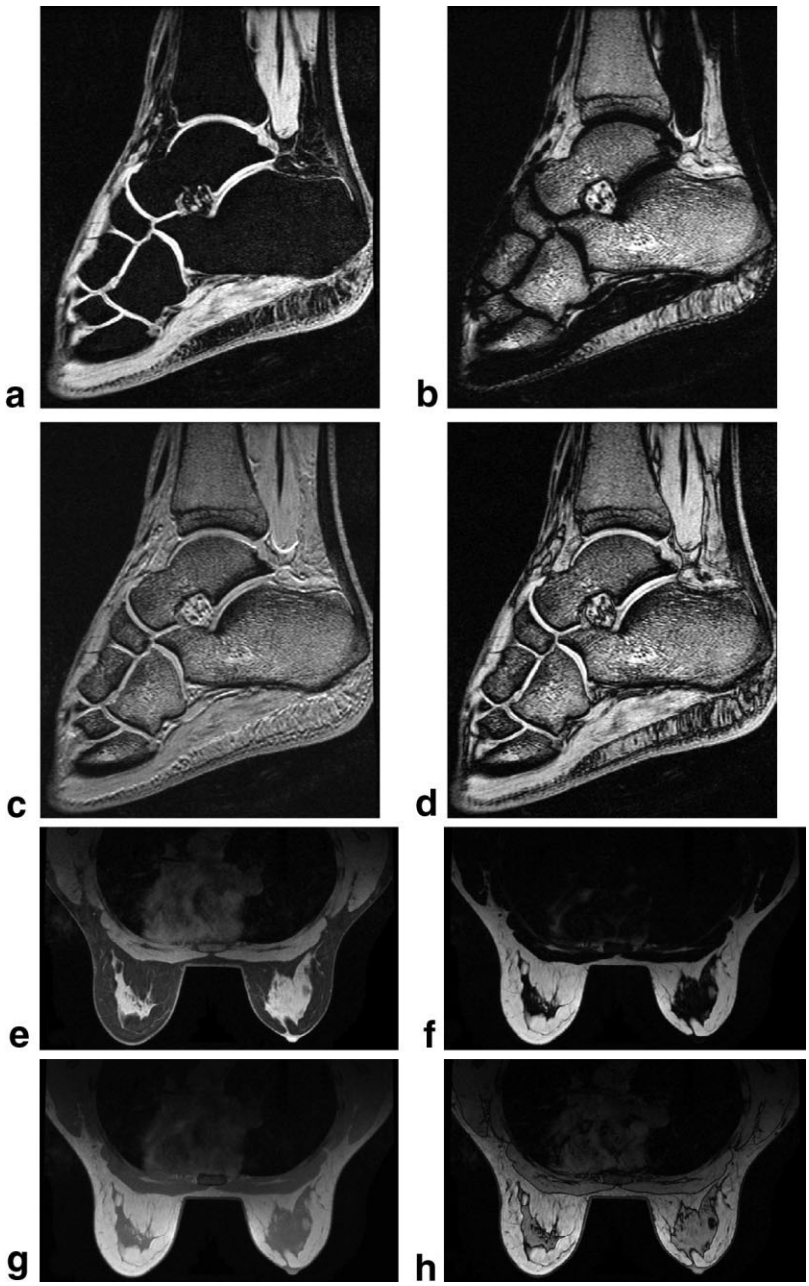

Figure 3. High-resolution sagittal 3D-IDEAL-SPGR water, fat, and recombined in-phase (water+fat) and out-of-phase (water–fat) images from the ankle of a normal volunteer acquired at 3.0T (**a–d**), and from the breasts of a normal volunteer at 1.5T (**e–f**). Uniform water–fat separation is seen throughout all images in both studies.

for FSE (11,12) with an asymmetric NSA curve; however, the broad minimum of the GRE data appears somewhat wider. This may have occurred because the theoretical predictions for NSA assumed very high-SNR source images, and the prior experiments were made with FSE images that had very high SNR. Regardless, the data from the quadrature echo combination show good agreement with the theoretical maximum of 3 for all fat: water ratios, and demonstrate tremendous improvement from the aligned echo combination.

The theoretical work by Pineda et al (11) also showed that the spacing between the echoes could also be other multiples of $2\pi/3$. For example, spacing between echoes of $4\pi/3$ or $8\pi/3$ (but not $6\pi/3 = 2\pi$) would also provide the optimum noise performance. For echoes acquired in different TRs, combinations with longer spacing than necessary should be avoided to avoid effects of T_2*. Longer echo spacing may be useful for multiecho water–fat separation methods, such as that described by Wieben (17), to increase the sequence flexibility and allow the long readout windows that are necessary for low-BW and/or large-matrix imaging.

IDEAL is a highly SNR-efficient method. It uses the information acquired in the source images very efficiently in the estimation of the calculated water and fat images. In fact, IDEAL is much more efficient than applications that use conventional fat saturation pulses, because the decrease in sequence efficiency from echo shifting is less than the time required to execute fat-saturation pulses. However, IDEAL requires a longer minimum scan time based on the need to acquire three images with different TEs. This makes IDEAL particularly well suited for applications that already use multiple averages, such as cartilage imaging,

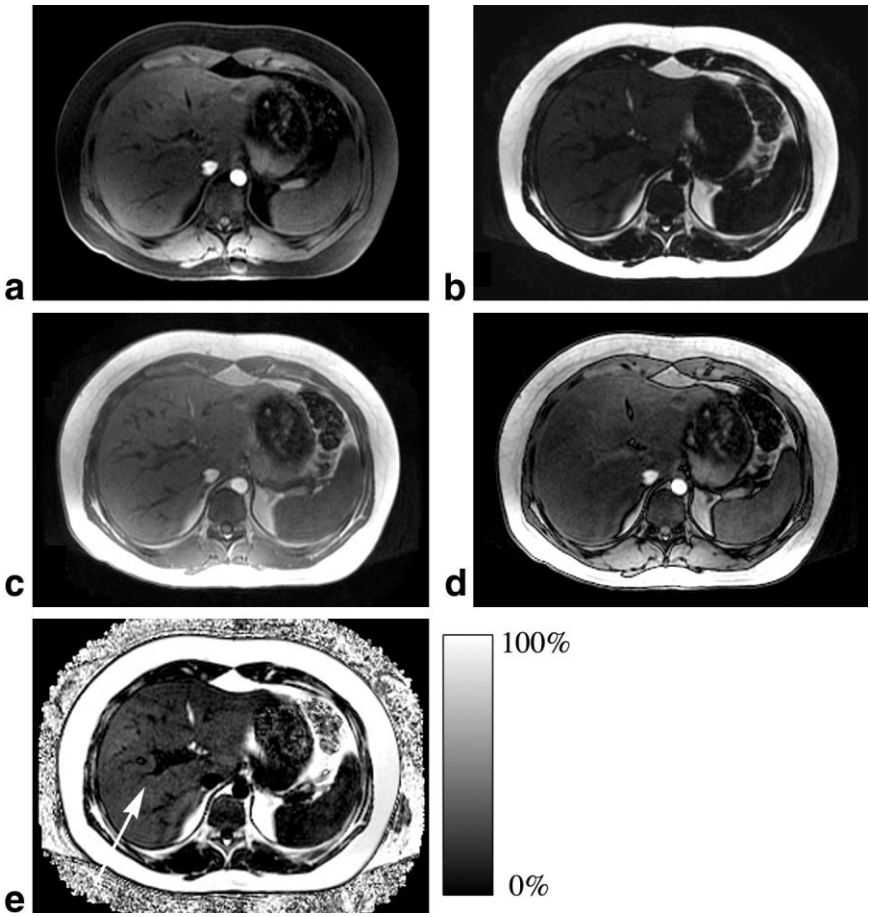

Figure 4. IDEAL-SPGR (**a**) water, (**b**) fat, (**c**) recombined in-phase, and (**d**) out-of-phase fat images acquired at 3.0T in a patient with fatty liver. Low-level signal is seen within the liver in the fat image, and signal dropout is also seen in the out-of-phase calculated image relative to the in-phase calculated image. **e:** The fat fraction (fat/(water+fat)) image demonstrates approximately 20% fat signal within the liver (arrow). Voxels = 1.5 × 2.7 × 7 mm^3; breath-hold time = 21 seconds.

where the limiting factors of conventional fat-saturated SPGR are SNR and image resolution (3). Improving sequence efficiency permits improved SNR and/or image resolution within the same scan time.

It is important to emphasize that because IDEAL can use arbitrarily spaced echoes, other echo combinations can be used, and small deviations from the optimal echo choices will have a minimal impact on noise performance if these deviations are small (11). This increased flexibility may be valuable for cases in which TE_{min} just exceeds the minimum TE of a particular echo group. In addition, echo flexibility is critical for cardiac IDEAL-SPGR applications in order to maintain short TRs and hence adequate temporal resolution. For most GRE applications, speed and sequence efficiency are the most important priorities, and the shortest echo group is chosen; however, one can easily generate T_2*W images by increasing the echo group index.

With separate water and fat images, a variety of new image combinations can be generated. Recombined images can be generated with the simple sum and difference of the calculated water and fat images, analogously to conventional "in-phase" and "out-of-phase" images that are commonly acquired for adrenal and liver imaging. This is also beneficial for distinguishing between benign lesions of the bone from metastases, since benign lesions contain fat and show decreased signal with out-of-phase imaging. Other possible calculated images, such as a "fat fraction" image (i.e., fat/(water+fat)) or a "fat: water ratio" image (i.e., fat/water) may be beneficial, particularly for quantitative applications such as characterization of hepatic steatosis and microscopic fat seen in adrenal adenomas, and possibly other entities. True quantitative measures of fat content will require knowledge of relaxation parameters within these tissues in order to yield absolute measures of fatty infiltration.

Chemical shift artifact can be corrected with IDEAL because the water and fat have been separated into different images that can be realigned. Chemical shift correction is routinely performed in the IDEAL reconstruction and presents a new opportunity for improved SNR performance by imaging at lower BWs and higher field strengths without increases in BW, while avoiding chemical shift artifact in the recombined images. Typically, the lower limit of image BW is determined by the level of chemical shift artifact. We routinely correct for chemical shift artifact with IDEAL.

IDEAL is particularly well suited for imaging at 3.0T because the chemical shift between water and fat doubles from approximately –210 Hz at 1.5T to –420 Hz. As a result, the spacing between echoes is reduced by half. This improves the overall efficiency of the pulse sequence by reducing the minimum TR of the sequence. In addition, the spacing between consecutive echo groups is also smaller (1.2 msec at 3.0T vs. 2.4 msec at 1.5T), which also improves sequence efficiency and flexibility while still imaging with an optimal echo combination.

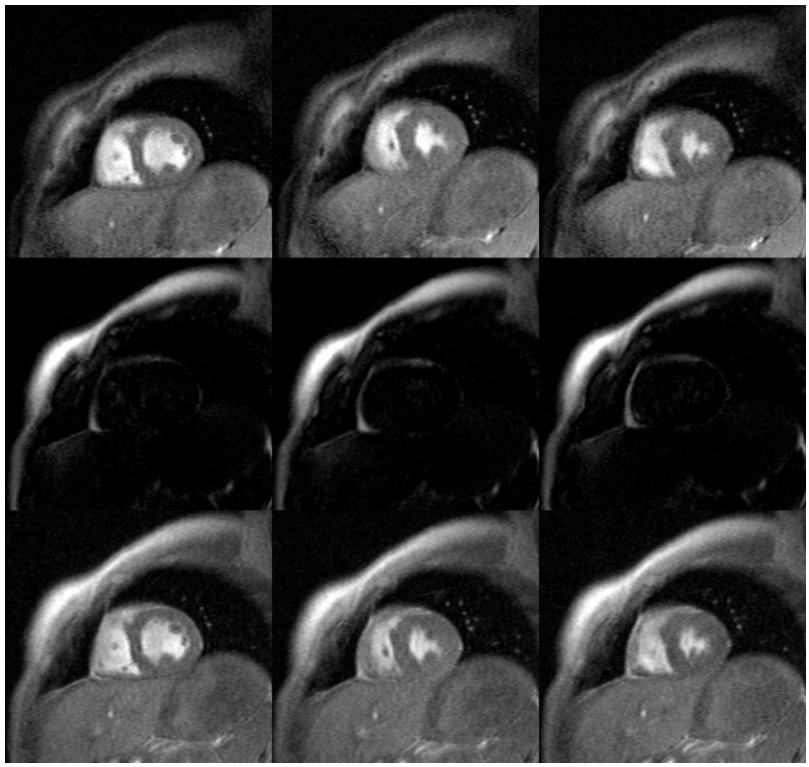

Figure 5. Three (of 20) cardiac CINE IDEAL-SPGR images acquired at 1.5T shown at end-diastole (left column), mid-systole (middle column), and end-systole (right column). Calculated water (top row), fat (middle row), and recombined in-phase (bottom row) images are shown, demonstrating uniform separation of water and fat across the image and throughout the cardiac cycle.

To prevent motion blurring caused by spatial misregistration of images acquired at different TEs, and therefore within different TRs, we interleaved the echoes for the three images. For each line of *k*-space, echoes at the three different TEs were sequentially acquired. In this way, the longest duration between lines of *k*-space for the three different TEs was 2 × TR (approximately 10–20 msec, depending on image parameters). In addition, the echoes were interleaved in such a way that the shortest TE (TE_1) was followed by the longest TE (TE_3) and finally the second echo (TE_2), to create the most equal spacing possible between the readout gradient waveforms. This echo ordering prevented the subtle ghosting artifacts that occurred when interleaved echoes were acquired in a sequential manner (i.e., TE_1, TE_2, TE_3).

The main disadvantage of IDEAL-GRE imaging is its long minimum scan time compared to that of conventional GRE imaging, which may be problematic for breath-held applications and dynamic contrast-enhanced imaging. Despite the increased scan time, IDEAL is a very SNR-efficient pulse sequence when the optimum echo spacing is used, and can generate separate water and fat images with SNR equivalent to three averages of a single image acquisition. For multicoil applications, this problem can be addressed in part by using parallel imaging accelerations. As shown in several examples above, parallel imaging is fully compatible with IDEAL water–fat decomposition. For low acceleration factors (R = 2–3), the SNR losses from the parallel acceleration are completely offset by the high SNR efficiency of IDEAL, which makes these methods highly complementary. Details of this work are described elsewhere (18). Other methods that can help reduce scan time include partial k_y and k_z acquisitions reconstructed with new homodyne algorithms that are compatible with IDEAL (19), as well as reduced acquisition schemes that include two-point (10) and single-point acquisition methods (20). Finally, we recently described the application of multiecho IDEAL acquisitions using EPI flyback readout gradients (21–23) that can reduce the scan time by a factor of 3. Other groups have published multiecho IDEAL methods in combination with SSFP imaging (17). Multiecho approaches work well at 1.5T for large-FOV applications such as liver imaging, but may be limited for small-FOV imaging (e.g., ankle) and imaging at 3.0T, in order to achieve optimal echo spacings. Regardless, the scanning principles described in this paper apply equally to both single- and multiecho IDEAL applications. Finally, it should be noted that scan-time reduction methods can be combined (e.g., multiecho IDEAL and parallel imaging) for even more substantial scan-time reductions (21).

In conclusion, we have demonstrated the feasibility of IDEAL water–fat separation in combination with GRE imaging, with optimization of the SNR performance and application to a variety of clinical applications.

ACKNOWLEDGMENT

The authors thank Jane W. Johnson, RT, for her assistance.

REFERENCES

1. Rofsky NM, Lee VS, Laub G, et al. Abdominal MR imaging with a volumetric interpolated breath-hold examination. Radiology 1999; 212:876–884.

2. Agoston A, Daniels B, Herfkens R, et al. Intensity-modulated parametric mapping for simultaneous display of rapid dynamic and high-spatial-resolution breast MR imaging data. Radiographics 2001;21:217–226.
3. Disler DG. Fat-suppressed three-dimensional spoiled gradient-recalled MR imaging: assessment of articular and physeal hyaline cartilage. AJR Am J Roentgenol 1997;169:1117–1123.
4. Bydder GM, Pennock JM, Steiner RE, Khenia S, Payne JA, Young IR. The short TI inversion recovery sequence—an approach to MR imaging of the abdomen. Magn Reson Imaging 1985;3:251–254.
5. Meyer CH, Pauly JM, Macovski A, Nishimura DG. Simultaneous spatial and spectral selective excitation. Magn Reson Med 1990;15: 287–304.
6. Dixon W. Simple proton spectroscopic imaging. Radiology 1984; 153:189–194.
7. Glover G. Multipoint Dixon technique for water and fat proton and susceptibility imaging. J Magn Reson Imaging 1991;1:521–530.
8. An L, Xiang QS. Chemical shift imaging with spectrum modeling. Magn Reson Med 2001;46:126–130.
9. Reeder SB, Wen Z, Yu H, et al. Multicoil Dixon chemical species separation with an iterative least-squares estimation method. Magn Reson Med 2004;51:35–45.
10. Ma J. Breath-hold water and fat imaging using a dual-echo two-point Dixon technique with an efficient and robust phase-correction algorithm. Magn Reson Med 2004;52:415–419.
11. Pineda A, Reeder S, Wen Z, Yu H, Pelc N. Cramer-Rao bounds for three-point decomposition of water and fat. Magn Reson Med 2005; 54:625–635.
12. Reeder S, Pineda A, Wen Z, et al. Iterative decomposition of water and fat with echo asymmetry and least-squares estimation (IDEAL): application with fast spin-echo imaging. Magn Reson Med 2005;54:636–644.
13. Fuller S, Reeder S, Shimakawa A, Yu H, Johnson J, Beaulieu CF, Gold GE. (IDEAL) FSE imaging of the ankle: initial experience. In: Proceedings of the 14th Annual Meeting of ISMRM, Seattle, WA, USA, 2006 (abstract 277).
14. Reeder S, Yu H, Johnson J, et al. T1 and T2 weighted fast spin-echo imaging of the brachial plexus and cervical spine with IDEAL water-fat separation. J Magn Reson Imaging 2006;24: 825–832.
15. Reeder S, Markl M, Yu H, Hellinger J, Herfkens R, Pelc N. Cardiac CINE imaging with IDEAL Water-fat separation and steady-state free precession. J Magn Reson Imaging 2005;22:44–52.
16. Yu H, Reeder S, Shimakawa A, Brittain J, Pelc N. Field map estimation with a region growing scheme for iterative three-point water-fat decomposition. Magn Reson Med 2005;54:1032–1039.
17. Wieben O, Leupold J, Mansson S, Hennig J. Multi-echo balanced SSFP imaging for iterative Dixon reconstruction. In: Proceedings of the 13th Annual Meeting of ISMRM, Miami Beach, FL, USA, 2005 (Abstract 2386).
18. McKenzie C, Reeder S, Shimakawa A, Pelc N, Brittain J. Abdominal three point Dixon imaging with self calibrating parallel MRI. In: Proceedings of the 12th Annual Meeting of ISMRM, Kyoto, Japan, 2004 (Abstract 917).
19. Reeder S, Hargreaves B, Yu H, Brittain J. Homodyne reconstruction for IDEAL water-fat decomposition. Magn Reson Med 2005;54: 586–593.
20. Yu H, Reeder SB, McKenzie CA, et al. Single acquisition water-fat separation: feasibility study for dynamic imaging. Magn Reson Med 2006;55:413–422.
21. Reeder S, Vu A, Hargreaves B, et al. Rapid 3D-SPGR imaging of the liver with multi-echo IDEAL. In: Proceedings of the 14th Annual Meeting of ISMRM, Seattle, WA, USA, 2006 (Abstract 2444).
22. Hargreaves B, Reeder S, Yu H, Shimakawa A, Brittain J. Flow independent angiography at 3.0T with dual-acquisition balanced SSFP and multi-echo IDEAL. In: Proceedings of the 14th Annual Meeting of ISMRM, Seattle, WA, USA, 2006 (Abstract 1940).
23. Gold G, Reeder S, Yu H, Brittain J, Hargreaves B. Multi-echo IDEAL water-fat separation for rapid imaging of cartilage. In: Proceedings of the 14th Annual Meeting of ISMRM, Seattle, WA, USA, 2006 (Abstract 632).